Ginsenoside Re attenuates homocysteine-induced endothelial cell ferroptosis through upregulation of GPX4/xCT signaling

SHAOLIN LI[1,2*], CHENGE ZHAO[2*], SHENGQIN YU[1], KAIJING YANG[1], SHUYING ZHANG[1] and SIXU LIU[1]

[1]Department of Cardiology, Affiliated Zhongshan Hospital of Dalian University, Dalian, Liaoning 116000, P.R. China;
[2]Department of Cardiology, The Fifth Affiliated Hospital of Jinan University, Heyuan, Guangdong 517000, P.R. China

Received June 1, 2025; Accepted October 17, 2025

DOI: 10.3892/etm.2025.13022

Abstract. Endothelial dysfunction is a key pathophysiological basis of atherosclerosis (AS). Potential mechanisms by which Hcy causes vascular injury include inhibiting endothelial cell growth, inducing endothelial dysfunction, and promoting vascular remodeling. Suppression of GPX4 synthesis can lead to exacerbated lipid peroxidation, triggering ferroptosis. The objective of the present study was to investigate whether ginsenoside Re attenuates homocysteine (Hcy)-induced endothelial cell ferroptosis by upregulating glutathione peroxidase 4 (GPX4). After treating EA.hy926 cells with different concentrations of Hcy for 24 h, cell viability was assessed using an MTT assay to determine the appropriate concentrations of Hcy for establishing a cell damage model. EA.hy926 cells were then divided into the following four groups: Control group, Hcy group, low-dose ginsenoside Re + Hcy group and high-dose ginsenoside Re + Hcy group. Cell viability was assessed using an MTT assay, whereas the BODIPY™ 581/591 C11 probe was used to measure cellular lipid peroxidation levels. Additionally, a 2',7'-dichlorodihydrofluorescein diacetate probe was used to measure the intracellular reactive oxygen species (ROS) content, while a microplate reader was used in combination with corresponding assay kits to measure the intracellular glutathione (GSH), malondialdehyde (MDA) and total iron ion levels. Furthermore, western blotting was conducted to determine the expression levels of GPX4, solute carrier family 7 member 11 (SLC7A11) and acyl-CoA synthetase long-chain family member 4 in the cells. Results demonstrated that high-dose and low-dose ginsenoside Re significantly alleviated the reduction in cell viability induced by Hcy and reduced the increase in ROS and lipid peroxide levels caused by Hcy. High concentrations of ginsenoside Re effectively mitigated the increase in MDA and total iron ion levels and the decrease in GSH levels induced by Hcy. Furthermore, western blotting results revealed that compared with the control group, the Hcy group exhibited lower expression levels of GPX4 and SLC7A11, while ACSL4 expression was elevated. By contrast, both low- and high-concentration ginsenoside Re significantly increased GPX4 and SLC7A11 expression levels and decreased ACSL4 expression levels compared with the Hcy group. In conclusion, ginsenoside Re significantly increased the expression levels of GPX4 in EA.hy926 cells and alleviated Hcy-induced endothelial cell ferroptosis. Ginsenoside Re may prevent microvascular endothelial dysfunction and subsequent tissue damage by reducing ferroptosis and protecting endothelial cells.

Correspondence to: Dr Sixu Liu or Dr Shuying Zhang, Department of Cardiology, Affiliated Zhongshan Hospital of Dalian University, 6 Jiefang Street, Zhongshan, Dalian, Liaoning 116000, P.R. China
E-mail: lau259259@163.com
E-mail: acezhangsy1868@163.com

*Contributed equally

Key words: ginsenoside Re, homocysteine, glutathione peroxidase 4, ferroptosis, endothelial cells

Introduction

Endothelial cell dysfunction serves as a key foundation for the pathophysiology of atherosclerosis (AS). Normal endothelial cells regulate the vascular tone, prevent thrombosis and modulate inflammation, serving key roles in maintaining vascular homeostasis and inhibiting AS (1). The initiation of AS involves endothelial apoptosis, ferroptosis and autophagy, among other programmed cell death mechanisms (2,3). Ferroptosis, a previously identified form of cell death, is distinct from apoptosis and autophagy and is characterized by molecular changes such as glutathione (GSH) depletion or GSH-peroxidase (GPX) inactivation, increased intracellular free iron levels and enhanced reactive oxygen species (ROS) generation, ultimately resulting in the accumulation of toxic lipid peroxides within cells (4-9). During ferroptosis, mitochondrial abnormalities such as condensation or swelling, increased membrane density, decreased or absent cristae and outer membrane rupture are commonly observed (10). Previous studies have indicated a close association between ferroptosis and various cardiovascular diseases, including AS (11), acute myocardial infarction (12), ischemia/reperfusion injury (13), cardiomyopathy and heart failure (14,15).

GPX4, one of the eight GPX proteins in mammals, is considered to be the only enzyme within cells capable of directly reducing phospholipid hydroperoxides. GPX4 converts lipid hydroperoxides into lipid alcohols, and the inhibition of GPX4

synthesis leads to exacerbated lipid peroxidation and subsequent ferroptosis (16,17). GSH serves as a key antioxidant in the body and acts as a co-factor for GPX4, participating in the reduction of lipid hydroperoxides (18). The depletion of GSH can result in GPX4 inactivation and increased production of intracellular lipid peroxides, ultimately triggering ferroptosis. Extracellular cystine is transported into cells through solute carrier family 7 member 11 (SLC7A11) with intracellular glutamate, which is then converted to the cysteine required for GSH synthesis. Inhibition of cystine uptake leads to reduced GSH synthesis, resulting in the accumulation of lipid peroxidation products and subsequent ferroptosis (19).

Homocysteine (Hcy) is a sulfur-containing amino acid, and high levels of homocysteine in the body can be attributed to factors such as the deficiency of methionine, folic acid, vitamin B12, B6 and B2 in the diet, and abnormal Hcy metabolic pathways. High levels of Hcy can lead to AS, hypertension and congestive heart failure, among other conditions (20,21). Hcy weakens vascular repair function through mechanisms such as oxidative stress, damage to the NO system and mitochondrial destruction, leading to vascular injury (22). A previous study indicated that Hcy can promote ferroptosis mediated by GPX4 methylation in nucleus pulposus cells and that folic acid intervention can reduce ferroptosis-related indicators induced by Hcy (23). However, studies on Hcy-induced endothelial cell ferroptosis are limited.

Ginsenoside Re, a dietary phytochemical (24), possesses advantages such as easy accessibility, low cost, efficient and simple purification techniques as well as low toxicity (25). Notably, ginsenoside Re exhibits various pharmacological effects, including antidiabetic (26), neuroregulatory (27), anti-infective (28), cardioprotective (29) and antitumor activities (30) and can alleviate the cellular oxidative stress response (31). However, studies on whether ginsenoside Re can inhibit ferroptosis are scarce. The present study aimed to establish a model of Hcy-induced endothelial cell damage and to investigate whether ginsenoside Re can suppress Hcy-induced endothelial cell ferroptosis by upregulating the expression of GPX4, thus providing a basis for the application of ginsenoside Re in anti-AS therapy (Fig. 1).

Materials and methods

Cell culture. The EA.hy926 cell line was purchased (cat. no. CL-0272; Procell®) and cultured in DMEM/F12 (cat. no. 11330032; Gibco; Thermo Fisher Scientific, Inc.) at 37˚C in a humidified incubator with 5% CO_2. All media contained 10% FBS (cat. no. LV-FBSCN500S; Ausgenex Pvt Ltd.), 100 U/ml penicillin and 100 μg/ml streptomycin (cat. no. C0222; Beyotime Biotechnology).

Cell toxicity assay. The cytotoxic effect of Hcy (cat. no. H4628; MilliporeSigma), ferroptosis inducers erastin (cat. no. HY-15763; MedChemExpress) and ginsenoside Re (cat. no. SG8310; Beijing Solarbio Science & Technology Co., Ltd.) on EA.hy926 cells was evaluated using an MTT assay at 37˚C. The cells were seeded at $1x10^5$ cells per well in a 96-well plate and allowed to adhere overnight. Subsequently, the cells were treated with different concentrations of Hcy (0-5 mM), erastin (0-20 μM) and ginsenoside Re (0-200 μM) in the culture medium for 48 h. Afterwards, 50 ml MTT was added and the resulting formazan crystals were dissolved in 150 μl DMSO. The absorbance was measured at 570 nm per well with a 96-well plate reader, and cell viability was expressed as the percentage of untreated controls. Our previous study demonstrated that exposure to Hcy (0-8 mM) resulted in a progressive reduction in cell viability from 100 to 30% (32). Consequently, in the present study, Hcy concentrations of 0-5 mM were selected.

Flow cytometry (FCM) to assess the cellular levels of lipid ROS (Lip-ROS). EA.hy926 cells were cultured overnight in a 6-well culture plate ($4x10^5$ cells/well). After discarding the culture medium from each well, cells were washed three times with PBS. Subsequently, the cells were treated with Hcy and ginsenoside Re and divided into the following four groups: The control group (untreated), the Hcy (2 mM) group, the Hcy (2 mM) + ginsenoside Re (12 μM) group and the Hcy (2 mM) + ginsenoside Re (24 μM) group. All groups were cocultured at 37˚C for 24 h. After 24 h of drug treatment, cell staining was performed. First, the culture medium was discarded from each well and 1 ml/well sterile PBS solution was added to remove any residual drugs. Subsequently, the pre-prepared BODIPY™ 581/591 C11 probe solution (cat. no. D3861; Thermo Fisher Scientific, Inc.) was diluted to 10 μM and 2 ml diluted probe solution was slowly added to each well of the 6-well plate. The plate was covered with aluminum foil and incubated in a 37˚C cell culture incubator for 30 min.

After incubation, the probe solution was aspirated and the cells were washed 2-3 times with sterile PBS. After washing, 0.5 ml EDTA-free trypsin was added to digest the cells and the plate was centrifuged at 415 x g at 37˚C for 5 min. After centrifugation, the supernatant was removed and 1 ml PBS solution was added to resuspend the cells. The resuspended cells were centrifuged at 415 x g at 37˚C for 5 min to remove as much residual trypsin digestion solution from the cell surface as possible. The residual solution in the tube was then removed and an appropriate amount of PBS buffer was added to resuspend the cells. The stained cells were transferred to a FCM tube and labeled, with all procedures conducted in the dark. Cell lipid peroxidation levels were measured using FCM with the BD FACSCalibur™ flow cytometer (BD Biosciences). A total of 10,000 gated events were recorded for each sample and analysis was performed using the BD FACSDiva™ software (version 8.0.1; BD Biosciences).

FCM to assess the intracellular levels of ROS. Experimental grouping and cell culture methods were performed as aforementioned. After 24 h of drug treatment, cell staining was performed. First, the culture medium was removed from each well and 1 ml/well sterile PBS solution was added to remove any residual drugs. Subsequently, the pre-prepared 2',7'-dichlorodihydrofluorescein diacetate probe solution (cat. no. S0033S; Beyotime Institute of Biotechnology) was diluted to 10 μM and 2 ml diluted probe solution was slowly added to each well of the 6-well plate. The plate was covered with aluminum foil and incubate in a 37˚C cell incubator for 30 min. Stained cells were then transferred to FCM tubes and labeled, with all procedures conducted in the dark. FCM was performed using the BD FACSCalibur flow cytometer to measure cellular ROS

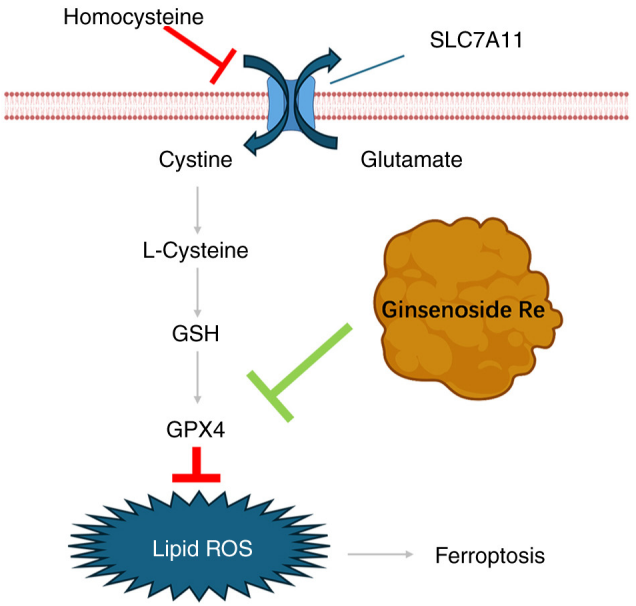

Figure 1. GPX4/SLC7A11 is a key pathway in ferroptosis. Homocysteine inhibition of the GPX4/SLC7A11 pathway leads to lipid peroxidation and promotes ferroptosis. Ginsenoside Re can attenuate lipid peroxidation by increasing the expression of GPX4 and protecting endothelial cells from ferroptosis. The red symbols indicate inhibition and the green symbol indicates promotion. GPX4, glutathione peroxidase 4; SLC7A11; solute carrier family 7 member 11; ROS, reactive oxygen species; GSH, glutathione.

levels. A total of 10,000 gated events were recorded for each sample and analysis was performed using the BD FACSDiva™ software (version 8.0.1).

Fluorescence detection of the levels of cellular Lip-ROS. After 24 h of drug treatment as aforementioned, cell staining was conducted. The initial steps of cell staining were the same as those for ROS detection. Subsequently, the cells were stained with Antifade Mounting Medium with DAPI (cat. no. P0131; Beyotime Institute of Biotechnology). Images were captured using a fluorescence microscope (x10 magnification; Olympus Corporation) in the dark. Quantitative analysis was performed using ImageJ software (version 1.54; National Institutes of Health).

Determination of intracellular total iron ion content. EA.hy926 cells were cultured overnight in 6-well plates ($4x10^5$ cells/well) and divided into four treatment groups as aforementioned, namely the control group, the Hcy (2 mM) group, the Hcy (2 mM) + ginsenoside Re (12 μM) group and the Hcy (2 mM) + ginsenoside Re (24 μM) group, with each group incubated for 24 h. After treatment, cells were collected and washed twice with cold sterile PBS, followed by low-speed centrifugation (37˚C, 415 x g, 5 min). PBS was then aspirated and 100-200 μl lysis buffer in the Total Iron Content Colorimetric Assay Kit (cat. no. E1042; Applygen Technologies, Inc.) was added. The cells were vigorously shaken or vortexed for 20-30 sec, then lysis was conducted at 4˚C for 2 h, before centrifugation at 4˚C at 12,000 x g for 5 min to collect the supernatant for subsequent determination of iron ion concentration and protein concentration was measured using a BCA assay. Preparation of the standard solution was then performed. A 3 mM standard solution was diluted with the dilution solution provided in the Total Iron Content Colorimetric Assay Kit to concentrations of 300, 150, 75, 37.5, 18.75, 9.38 and 4.69 μM. A mixture of reagent 2 and 4.5% potassium permanganate solution was prepared in a 1:1 ratio to form solution A. The blank control group, standard group and sample group were set up and mixed with solution A before being incubated in a water bath at 60˚C for 1 h. After the tubes cooled to room temperature, the liquid remaining on the wall and cap of the tubes was centrifuged at low speed (37˚C, 415 x g, 5 min) to the bottom of the tubes. Subsequently, 30 μl iron ion detection reagent, included in the aforementioned kit, was added and the mixture was incubated at room temperature for 30 min. After centrifugation at 4˚C at 12,000 x g for 5 min, the supernatant was collected. Finally, 200 μl sample was added to each well of a 96-well plate and the absorbance of the samples was measured at 550 nm using a microplate reader. The relative iron ion levels were checked in the cells.

Determination of the intracellular GSH concentration. The cells were ultrasonically crushed using PBS as the homogenizing medium and then centrifuged to take the supernatant for determination. A total of 0.1 ml cell supernatant was removed, and then 0.1 ml reagent 1 (precipitating agent) was added to the tube and thorough mixing was performed. The mixture was centrifuged at 37˚C at 205 x g for 10 min and the supernatant was collected for measurement. After the control group, Hcy group, low-dose ginsenoside Re + Hcy group and high-dose ginsenoside Re + Hcy group were treated with reagent 1, 100 μl reagent 2 (buffer solution) and 25 μl reagent 3 (color developer) were added to the supernatant, mixed and allowed to stand for 5 min. The absorbance of the samples was measured at 405 nm using a microplate reader. GSH standard solutions were prepared by diluting a GSH standard stock solution to concentrations of 100, 50, 20, 10, 5 and 0 μM. All reagents used were included in the GSH Assay Kit (cat. no. A006-2-1; Nanjing Jiancheng Bioengineering Institute). The GSH content was analyzed based on the measured absorbance values using a standard curve. Based on the absorbance measurement value, the relative GSH level was checked in the cells.

Determination of the intracellular malondialdehyde (MDA) content. To measure MDA content using an MDA kit (cat. no. A003-4-1; Nanjing Jiancheng Bioengineering Institute), 100 μl anhydrous ethanol, standard solution and test samples were mixed separately with 1,000 μl working solution to prepare control tubes, standard tubes and sample tubes, respectively. After thorough mixing, the tubes were heated in a water bath at >95˚C for 40 min. The solutions were then removed from the water bath and cooled under running water, before being centrifuged at 37˚C at 268 x g for 10 min. The optical density (OD) of the blank plate was measured at 530 nm using a microplate reader. Subsequently, 0.25 ml of each sample was transferred to a new 96-well plate and the OD value of each well was measured using a microplate reader (the OD value of the blank plate was subtracted from the sample OD value). The results were normalized to the percentage of the control group.

Molecular docking. Molecular docking evaluation of ginsenoside Re combined with different proteins was performed. Briefly, the 3D molecular structure of ginsenoside Re was retrieved from the PubChem database (https://pubchem.ncbi.nlm.nih.gov/). In addition, the X-ray crystal structures of the GPX4, SLC7A11 and acyl-CoA synthetase long-chain family member 4 (ACSL4) proteins were obtained from Protein Data Bank (http://www.rcsb.org/). For protein preparation, PyMOL (https://github.com/schrodinger/pymol-open-source) (version 2.5.2) was used to remove water molecules and heteroatoms and the proteins were saved in 'pdb format'. AutoDock (https://autodock.scripps.edu/download-autodock4/) (version 4.2.6) and PyMOL software were used to perform docking studies between ginsenoside Re and GPX4, SLC7A11 and ACSL4 proteins. The grid-box function of AutoDock Tools was used to define specific pockets of active ingredients for protein-protein interaction binding to proteins. Subsequently, molecular docking analysis was performed using the command prompt and the results were displayed using PyMOL. The default settings of the software were used.

Western blotting. Cells were seeded on a 6-well plate at $2.5x10^5$ cells/well and allowed to adhere overnight. Subsequently, the cells were incubated with Hcy (2 mM), Hcy (2 mM) + ginsenoside Re (12 μM) or Hcy (2 mM) + ginsenoside Re (24 μM) for 24 h, after which, the medium in the 6-well plate was discarded. Precooled PBS was then added to rinse the cells twice. A prepared protein lysis solution RIPA (cat. no. P0038; Beyotime Institute of Biotechnology) + PMSF (cat. no. ST507; Beyotime Institute of Biotechnology) (RIPA:PMSF, 100:1) was added to lyse the cells for 30 min at 4˚C (shaking the 6-well plate every 10 min), the cells were quickly collected with a cell scraper and centrifuged using a high-speed refrigerated centrifuge at 950 x g for 15 min at 4˚C. The supernatant was aspirated and a BCA protein assay kit was used to determine the total protein concentration. Subsequently, western blotting of the lysates was performed. Equal amounts of protein (20 μg per lane) were electrophoresed on 10% SDS-polyacrylamide gels and transferred onto 0.45 μm PVDF membranes. The membranes were then blocked with 5% skimmed milk for 1 h at room temperature, followed by an overnight incubation with the primary antibody at 4˚C. The primary antibodies used included anti-GPX4 (1;2,000; cat. no. ab125066; Abcam), anti-SLC7A11 (1;2,000; cat. no. ab300667; Abcam), anti-ACSL4 (1;2,000; cat. no. ab155282; Abcam) and anti-GAPDH (1:2,000; cat. no. ab8245; Abcam). Following washes with TBST buffer (0.05% Tween-20), the membranes were incubated with horseradish peroxidase-conjugated secondary antibodies (1;5,000; cat. no. XD345904; Thermo Fisher Scientific, Inc.) at 37˚C for 60 min. The immunoreactive bands were then detected using an Odyssey CLX imaging system (LI-COR, Inc.), and Image Studio™ software (LI-COR, Inc.) was used to measure the OD of the bands.

Statistical analysis. All data are presented as the mean ± SD of at least three independent experiments, and the data were analyzed with GraphPad Prism (version 5.0; GraphPad; Dotmatics). For comparisons involving three or more groups, a one-way ANOVA was conducted, followed by Tukey's post-hoc test to assess significance. $P<0.05$ was considered to indicate a statistically significant difference.

Results

Hcy may induce ferroptosis in EA.hy926 endothelial cells. EA.hy926 cells were seeded into a 96-well plate and treated with different concentrations of Hcy for 24 h. Results indicated a gradual decrease in cell viability with increasing concentrations of Hcy (Fig. 2A). Subsequently, HCY were selected with a cell viability close to the IC_{50} at a concentration of 2 mmol (cell viability, 60%) and the lowest cell viability at 5 mmol (cell viability, 20%) for the subsequent western blotting experiment. Western blotting was conducted on cells treated with 2 or 5 mM Hcy for 24 h to detect expression of the ferroptosis-related proteins GPX4, SLC7A11 and ACSL4 (Fig. 2B) (32). Results demonstrated that the expression levels of GPX4 and SLC7A11 decreased with increasing Hcy concentration, while the expression levels of ACSL4 increased with increasing Hcy concentration, potentially indicating an increase in ferroptosis in EA.hy926 cells in response to increasing Hcy concentration (Fig. 2C). Furthermore, EA.hy926 cells treated with 2 or 5 mM Hcy for 24 h were stained with the diluted BODIPY 581/591 C11 probe for lipid peroxidation detection through inverted fluorescence microscopy (Fig. 2D). With increasing Hcy concentration, the intensity of green fluorescence within the cell markedly increased, further suggesting that Hcy induces ferroptosis in EA.hy926 cells.

Ginsenoside Re may mitigate erastin-induced ferroptosis in endothelial cells. To validate the impact of ginsenoside Re on cell viability, different concentrations of ginsenoside Re were applied to EA.hy926 cells for 24 h (Fig. 3A). Results indicated that ginsenoside Re had no significant effect on EA.hy926 cell viability. Erastin, an activator of ferroptosis, was used at various concentrations to treat EA.hy926 cells for 24 h, resulting in decreased cell viability with increasing concentrations of erastin (Fig. 3B). Erastin at a drug concentration of 5 μM with a cell viability of 50% was selected for subsequent experiments. For the convenience of concentration calculation, cells were treated with 12 μM or 24 μM of ginsenoside Re (Fig. 3C), with increasing concentrations of ginsenoside Re notably improving cell viability. These findings suggested that ginsenoside Re alleviated erastin-induced endothelial cell ferroptosis in a dose-dependent manner. After treatment with 12 or 24 μM ginsenoside Re for 24 h, western blotting was performed (Fig. 3D and E) and the results showed that the expression level of GPX4 increased after the addition of ginsenoside Re.

Ginsenoside Re may alleviate Hcy-induced endothelial cell ferroptosis. To validate the impact of ginsenoside Re on the cell damage caused by Hcy, EA.hy926 cells were treated with 2 mM Hcy and with 12 or 24 μM ginsenoside Re. Results demonstrated that the addition of ginsenoside Re could mitigate the cell damage caused by Hcy, as the reduction in cell viability caused by Hcy was reversed with increasing concentrations of ginsenoside Re (Fig. 4A). Intracellular ROS levels were measured using FCM, which revealed an increase in ROS levels in the Hcy-treated groups. Ginsenoside Re markedly reduced the increase in ROS concentration induced by Hcy (Fig. 4B). Using a microplate reader, intracellular iron ion, GSH and MDA levels were measured. Results

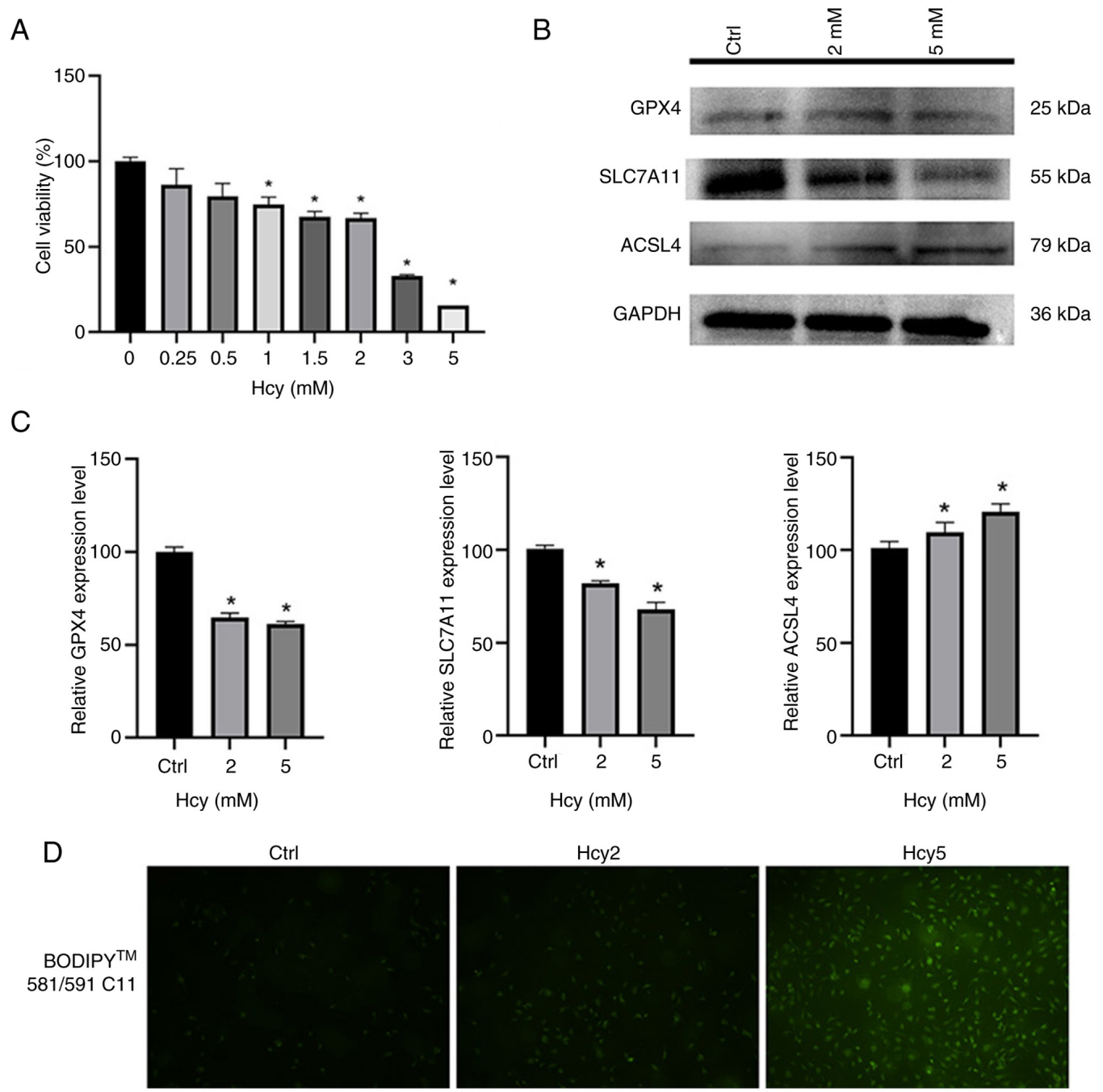

Figure 2. Hcy induces ferroptosis in EA.hy926 endothelial cells. (A) Effect of 0-5 mM Hcy on the viability of EA.hy926 cells as detected by MTT assay. (B) Expression levels of GPX4, SLC7A11 and ACSL4 detected by western blotting after treatment of EA.hy926 cells with 2 or 5 mM Hcy for 24 h, (C) with the optical density of the proteins calculated. (D) Cells were stained with the BODIPY 581/591 C11 probe and lipid peroxidation levels were detected by inverted fluorescence microscopy (x10 magnification). Data are presented as the mean ± SD. *P<0.05 vs. Ctrl. GPX4, glutathione peroxidase 4; SLC7A11; solute carrier family 7 member 11; ACSL4, acyl-CoA synthetase long-chain family member 4; Hcy, homocysteine; Ctrl, control.

revealed that Hcy could increase the levels of Fe^{2+} and MDA, while decreasing GSH levels in cells compared with those in the control group. By contrast, ginsenoside Re decreased the levels of Fe^{2+} and MDA, while increasing GSH levels compared with those in Hcy-treated cells (Fig. 4C-E). These findings suggested that ginsenoside Re alleviates Hcy-induced endothelial cell ferroptosis.

Effect of ginsenoside Re on Lip-ROS levels in EA.hy926 cells. After EA.hy926 cells were treated with 2 mM Hcy and either 12 or 24 μM ginsenoside Re, the BODIPY 581/591 C11 probe was added for staining. Fluorescence microscopy and FCM were used to measure the level of lipid peroxidation in cells. After Hcy treatment, the fluorescence intensity of the cells increased, whereas the fluorescence intensity decreased in the groups treated with ginsenoside Re compared with that treated with Hcy alone. These results indicate that Hcy increased the Lip-ROS level in the cells, while a low dose of ginsenoside Re had no significant effect on the Lip-ROS level in Hcy group cells. High-dose ginsenoside Re reduced Lip-ROS levels (Fig. 5A and B). Subsequently, it was shown through flow cytometry that the Hcy group could increase the intracellular

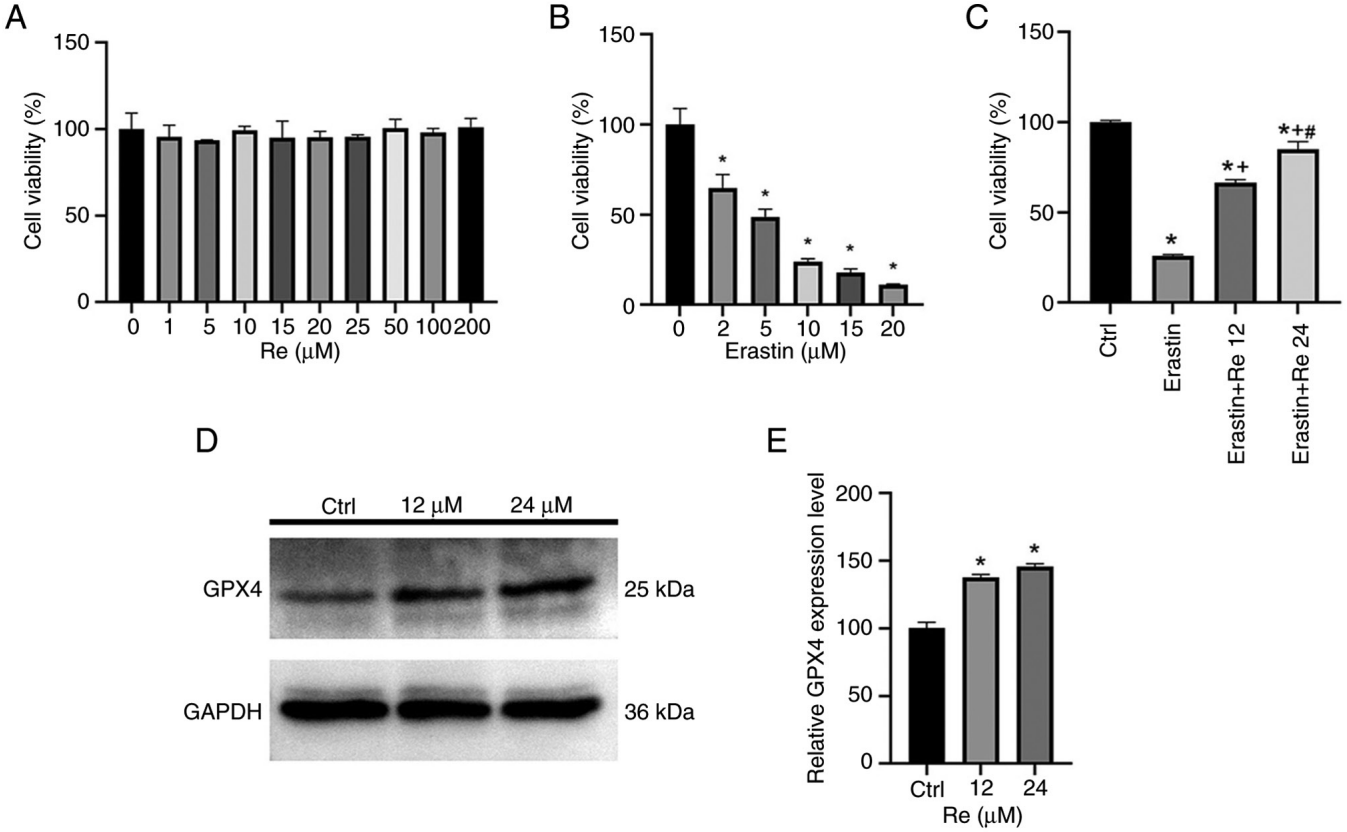

Figure 3. Ginsenoside Re attenuates erastin-induced endothelial cell ferroptosis. (A) Effects of 0-200 μM ginsenoside Re on the viability of EA.hy926 cells detected by MTT assay. (B) Erastin (0-20 μM) was added to EA.hy926 cells and cell viability was detected by MTT assay. (C) EA.hy926 cells were co-incubated with 5 μM erastin or 5 μM erastin + 12 or 24 μM ginsenoside Re for 24 h and cell viability was determined using an MTT assay. (D) Representative bands and (E) quantification analysis showing protein levels of GPX4 determined by western blotting with the optical density of the proteins calculated. Data are presented as the mean ± SD. *P<0.05 vs. Ctrl, $^{+}$P<0.05 vs. Erastin, $^{\#}$P<0.05 vs. Erastin + Re 12. GPX4; glutathione peroxidase 4; Ctrl, control; Re, ginsenoside Re.

Lip-ROS level, and the low-dose ginsenoside Re (12) intervention could reduce the reactive oxygen species level, but the rate was still higher than that of the control group. The high-dose ginsenoside re group (24) could reduce Lip-ROS levels to normal levels (Fig. 5C and D).

Association between ginsenoside Re and the GPX4, SLC7A11 and ACSL4 antioxidant axis. To elucidate the mechanism by which ginsenoside Re reduces ferroptosis in EA.hy926 cells, the effect of ginsenoside Re on the GPX4, SLC7A11 and ACSL4 antioxidant axis in ferroptosis was evaluated. Previous studies have reported that protein binding to ligands is influenced by binding energies, with binding energies <-5.0 kcal/mol indicating good binding and those <-7.0 kcal/mol indicating very firm binding (33,34). Docking results showed that the binding energies of ginsenoside Re with GPX4, SLC7A11 and ACSL4 were all <-7.0 kcal/mol (Table I). To more intuitively reflect the combination of active ingredients and key targets, PyMOL was used to visualize the results, revealing amino acid residues and the combination of hydrogen bonding and active compounds. Therefore, active components that bind strongly to target proteins were selected for visualization (Fig. 6). The results revealed that ginsenoside Re binds to GPX4 on amino acid residues methionine (MET)-102 and lysine (LYS)-99 (Fig. 6A), to ACSL4 on amino acid residues aspartate (ASP)-66, arginine (ARG)-60, glycine (GLY)-523, glutamine (GLN)-524 and histidine (HIS)-291 (Fig. 6B) and to SLC7A11 on amino acid residues GLN-438, ASP-350 and ARG-440 (Fig. 6C). These findings suggested a direct association between ginsenoside Re and the GPX4, SLC7A11 and ACSL4 antioxidant axis.

Impact of ginsenoside Re on the expression of ferroptosis-related proteins induced by Hcy in EA.hy926 cells. The present study indicated that after Hcy treatment of cells, the expression levels of GPX4 and SLC7A11 proteins decreased. After treating EA.hy926 cells with 12 and 24 μM ginsenoside Re, it was found that the expression levels of GPX4 and SLC7A11 increased compared with the Hcy alone group, indicating that ginsenoside Re treatment could significantly increase the expression level of ferroptosis protein induced by Hcy. The ferroptosis protein marker ACSL4 was significantly increased in the Hcy group, but significantly decreased in the ginsenoside Re groups, thus suggesting that ginsenoside Re may alleviate Hcy-induced endothelial cell ferroptosis (Fig. 7A and B). The present study demonstrated that ginsenoside Re significantly increased the expression levels of GPX4 in Hcy-treated EA.hy926 cells and therefore may mitigate Hcy-induced ferroptosis in EA.hy926 cells. The results of this study have clinical application value for the

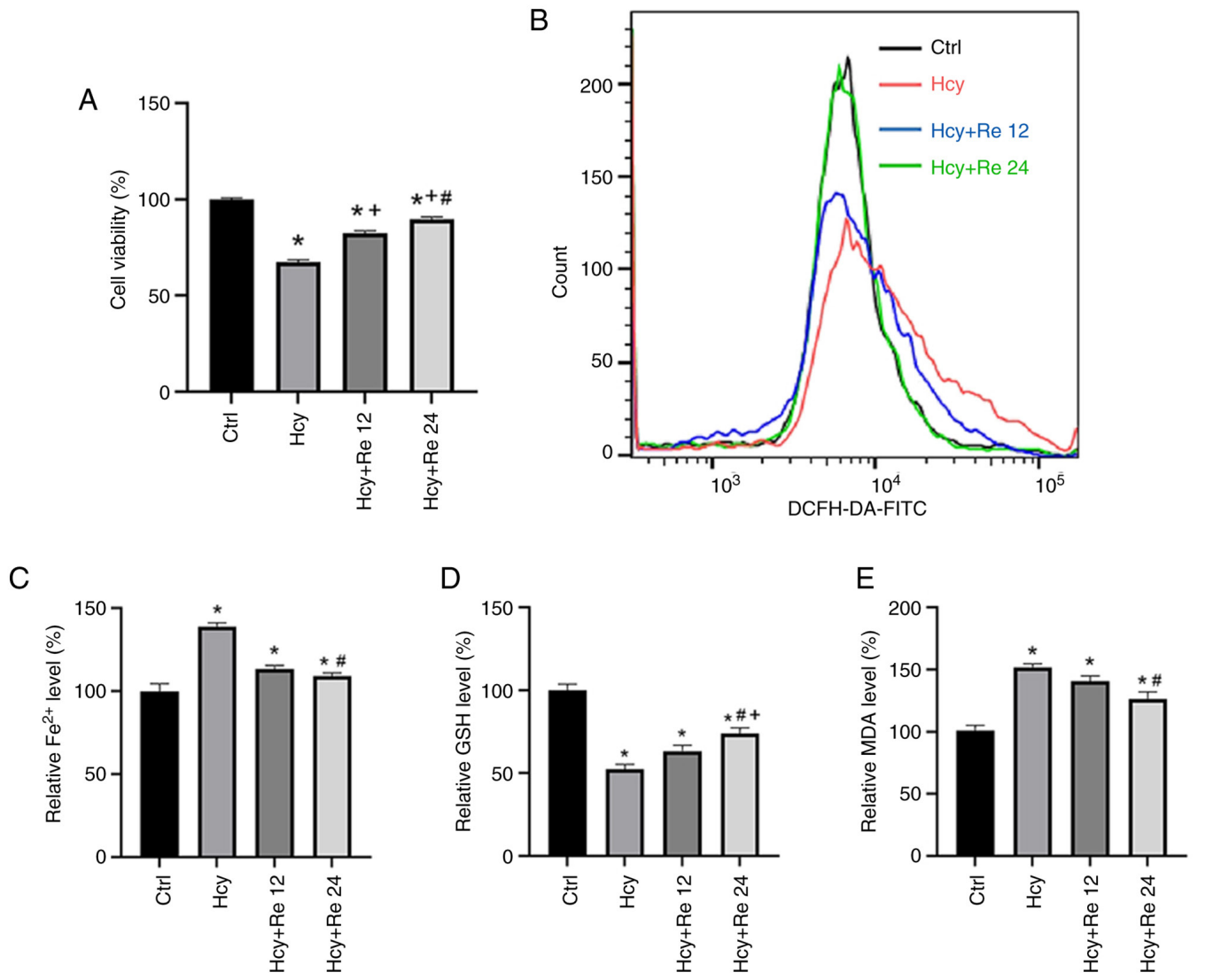

Figure 4. Ginsenoside Re alleviates Hcy-induced endothelial cell ferroptosis. (A) Hcy (2 mM), Hcy (2 mM) + ginsenoside Re (12 μM) and Hcy (2 mM) + ginsenoside Re (24 μM) were added to EA.hy926 cells and the cell viability was determined. (B) Flow cytometric analysis of intracellular reactive oxygen species levels in EA.hy926 cells. Detection of intracellular (C) iron ion, (D) GSH and (E) MDA levels in EA.hy926 cells. Data are presented as the mean ± SD. *P<0.05 vs. Ctrl; +P<0.05 vs. Hcy; #P<0.05 vs. Hcy + Re 12. Hcy, homocysteine; Ctrl, control; GSH, glutathione; MDA, malondialdehyde; Re, ginsenoside Re; DCFH-DA, 2',7'-dichlorodihydrofluorescein diacetate.

treatment of AS caused by endothelial cell injury resulting from ferroptosis.

Discussion

Ferroptosis serves a key role in the progression of AS, participating in various pathological processes, such as endothelial cell damage, macrophage inflammation, foam cell formation and vascular smooth muscle cell proliferation and migration (35-38), making ferroptosis a novel target for AS research. Therefore, exploring the relevant mechanisms of endothelial cell ferroptosis and identifying effective intervention methods are key in the treatment of AS.

Hcy is an independent risk factor for cardiovascular disease. Increased levels of Hcy can damage endothelial cells, leading to local infiltration of lipids and inflammatory cells and the formation of foam cells and lipid streaks, which gradually progress to atherosclerotic plaques (20,39). In recent years, a number of studies have demonstrated the involvement of ferroptosis in cell damage caused by Hcy; for example, a study found that the protective properties of Fer-1 against KGN cell Hcy-induced injury were mediated by TET activity and DNA demethylation (40). Wang *et al* (41) reported that Hcy may promote pulmonary microvascular endothelial cell ferroptosis by upregulating ACSL4 and downregulating GPX4 and ferroptosis suppressor protein 1 expression. The present study showed that the expression levels of GPX4 and SLC7A11 were lower in Hcy-treated EA.hy926 cells than those in the control group, while the expression levels of ACSL4 and the levels of Lip-ROS were greater than those in the control group. These results indicated that Hcy could decrease the expression of GPX4 and SLC7A11, potentially leading to increased Lip-ROS generation and therefore endothelial cell ferroptosis.

It has been shown that ginsenoside Re can upregulate the expression of GPX4 in cells through a process mediated by phosphoinositide 3-kinase and extracellular signal-regulated

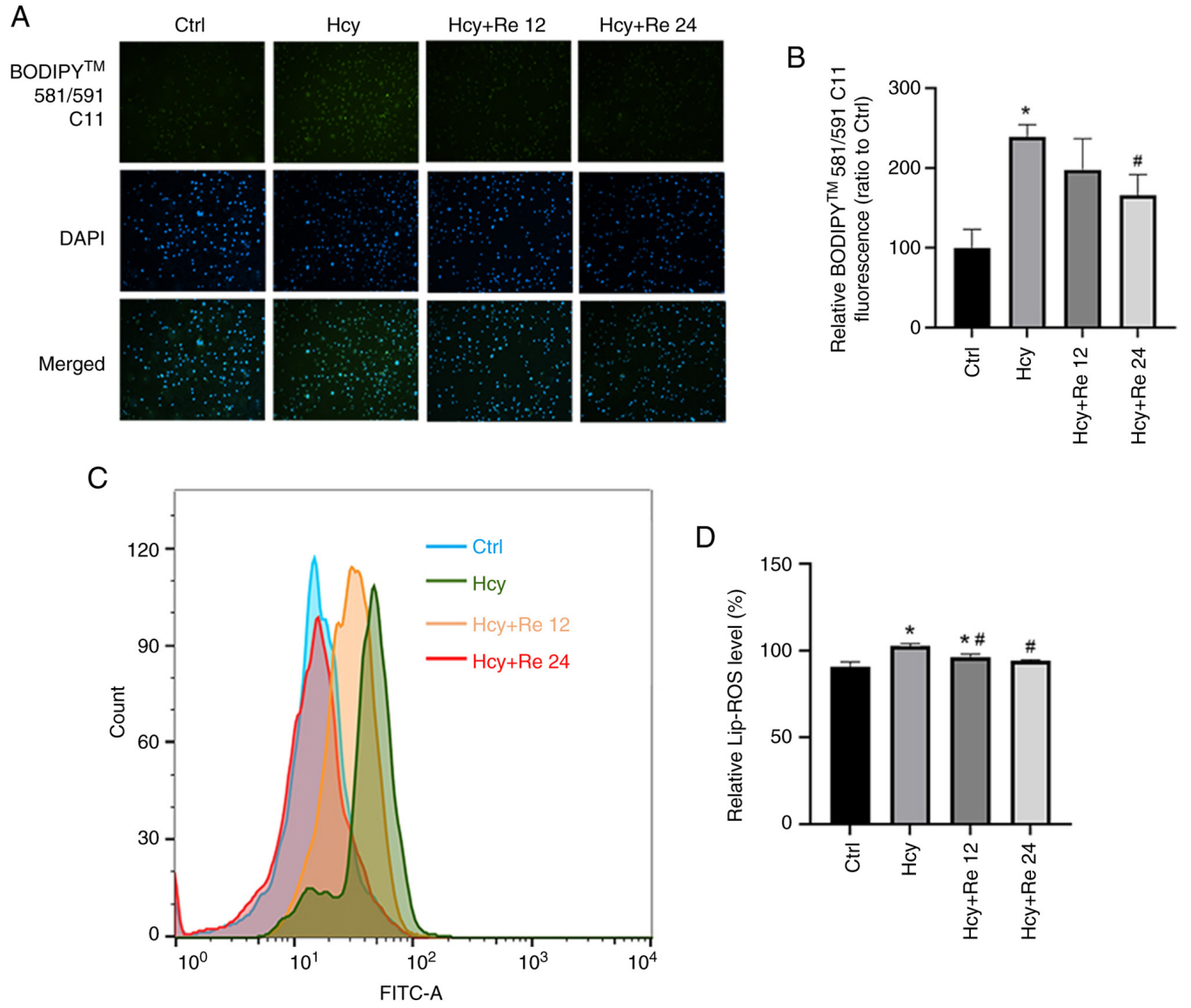

Figure 5. Effect of ginsenoside Re on Lip-ROS levels in EA.hy926 cells. (A) Images (x10 magnification) and (B) analysis of the detection of Lip-ROS levels through fluorescence microscopy after cotreatment of EA.hy926 cells with Hcy and ginsenoside Re for 24 h. (C) Flow cytometry plots and (D) analysis of the detection of Lip-ROS levels in EA.hy926 cells. Data are presented as the mean ± SD. *P<0.05 vs. Ctrl; #P<0.05 vs. Hcy. Lip-ROS, lipid reactive oxygen species, Hcy, homocysteine; Ctrl, control; Re, ginsenoside Re.

kinase, thereby alleviating oxidative stress-induced neuronal damage (31). In a previous study, 10-50 μM ginsenoside Re alone was applied to SH-SY5Y cells for 9 h, which markedly increased the expression levels of GPX4 in a concentration-dependent manner (31). The present study showed that within a certain concentration range (0-200 μM), ginsenoside Re had no significant effect on cell viability. After treating EA.hy926 cells with ginsenoside Re at concentrations of 12 and 24 μM for 24 h, the expression levels of GPX4 were increased compared with those in the control group. Ye *et al* (42) pretreated rats with 150 mg/kg ginsenoside Re for 5 days, after which a myocardial ischemia/reperfusion injury model was generated. This previous study revealed that ginsenoside Re alleviated myocardial cell ferroptosis induced by ischemia/reperfusion injury through microRNA (miR)-144-3p and SLC7A11. These findings suggest that ginsenoside Re may increase the expression levels of GPX4 and exert a protective effect on ferroptosis in various cell types at appropriate concentrations and treatment durations.

Since the discovery of ferroptosis, there has been a focus on its two major regulatory mechanisms, namely the disturbance in iron metabolism and lipid peroxidation. The Fenton reaction refers to the process where Fe^{2+} reacts with hydrogen peroxide to generate Fe^{3+} and oxygen radicals. Excessive iron within cells can generate oxygen radicals and ROS through the iron-dependent Fenton reaction, activating iron-containing enzymes such as lipoxygenase, and leading to oxidative stress and lipid peroxidation, thereby triggering ferroptosis (43). In 2012, Dixon *et al* (10) stimulated HT1080 cells with erastin, which resulted in a marked increase in intracellular iron ion and Lip-ROS levels. Notably, intervention with iron chelators and lipid peroxidation inhibitors markedly improved cell viability. Chen *et al* (44) established a ferroptosis model in H9C2 cells by stimulating them with artemisinin for 24 h. Fluorescence

Table I. Docking analysis between ginsenoside Re and target proteins.

Compound	Key target	Protein Data Bank ID	Binding energy (kcal/mol)
Ginsenoside Re	GPX4	6HN3	-12.8
	SLC7A11	7EPZ	-13.1
	ACSL4	AF_AFO60488F1	-12.8

GPX4, glutathione peroxidase 4; SLC7A11, solute carrier family 7 member 11; ACSL4, acyl-CoA synthetase long-chain family member 4.

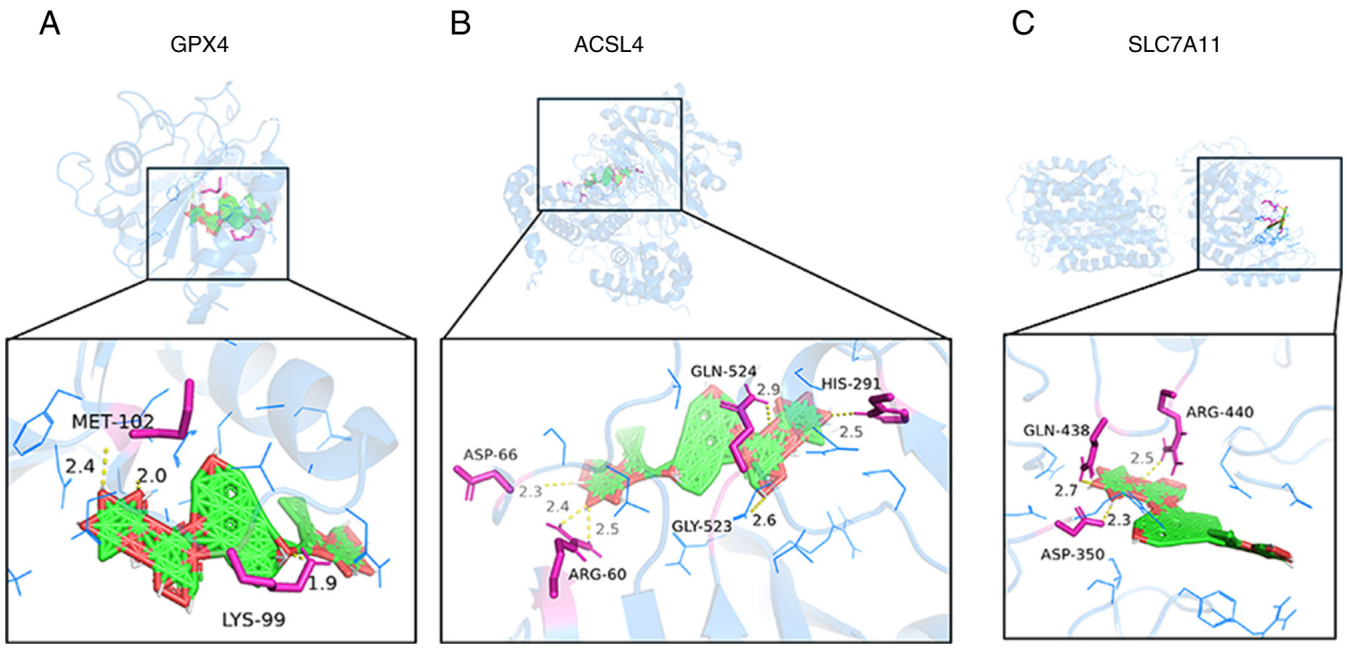

Figure 6. Optimal docking map of ginsenoside Re and key gene molecules. Ginsenoside Re can bind to (A) GPX4, (B) ACSL4 and (C) SLC7A11. The yellow dotted line represents hydrogen bonds, and the number beside the dotted line indicates the length of the hydrogen bond in Ångströms. GPX4, glutathione peroxidase 4; SLC7A11; solute carrier family 7 member 11; ACSL4, acyl-CoA synthetase long-chain family member 4; MET, methionine; LYS, lysine; ASP, aspartate; ARG, arginine; GLY, glycine; GLN, glutamine; HIS, histidine.

microscopy revealed marked increases in intracellular ROS and Fe^{2+} levels as well as lipid peroxidation. By contrast, SLC7A11 overexpression or miR-16-5p knockdown inhibits ferroptosis and exhibits cardioprotective effects *in vitro* and *in vivo*. The present study revealed that Hcy can lead to a significant increase in the levels of ferroptosis related factors Fe^{2+}, MDA and ROS. However, after the intervention with ginsenoside Re, the levels of Fe^{2+}, ROS, Lip-ROS and MDA were all lower than those in the Hcy group. These findings suggested that ginsenoside Re treatment potentially reduced the occurrence of the Fenton reaction, decreased cellular lipid peroxidation levels and thereby alleviated Hcy-induced endothelial cell ferroptosis.

Cystine/glutamate antiporter (system xc^-)/GPX4 is an important antioxidant system and one of the central mechanisms underlying ferroptosis (45). System xc^- consists of a light chain subunit (xCT, also known as SLC7A11) and a heavy chain (hc) subunit (CD98hc, also known as solute carrier family 3 member 2) located on the cell membrane (46). Extracellular cystine is absorbed into cells in equimolar amounts and rapidly reduced to cysteine, participating in the synthesis of the important intracellular free radical scavenger GSH (47). GSH is an essential antioxidant in cells that is synthesized by cysteine synthase and GSH synthetase and is also a key neurotransmitter and endogenous antioxidant in the body (48). System xc^- participates in the biosynthesis of GSH, and GSH, as an important cofactor of GPX4, reduces intracellular oxygen levels. When system xc^- is inhibited by certain compounds (such as erastin), GSH synthesis is decreased, leading to the inability of GPX4 to use GSH to reduce lipid peroxides, resulting in ferroptosis. To evaluate the extent to which ginsenoside Re binds ferroptosis-related proteins, the present study performed molecular docking experiments with GPX4, ACSL4, SLC7A11 and ginsenoside Re. Results showed that ginsenoside Re tightly bound to the three target proteins. Notably, the binding energies of ginsenoside Re to GPX4, ACSL4 and SLC7A11 were all <-7.0 kcal/mol, indicating a strong binding affinity. Molecular docking analysis of ginsenoside Re with the ferroptosis-related proteins GPX4, ACSL4 and SLC7A11 revealed key interactions, suggesting their potential therapeutic relevance. The interaction

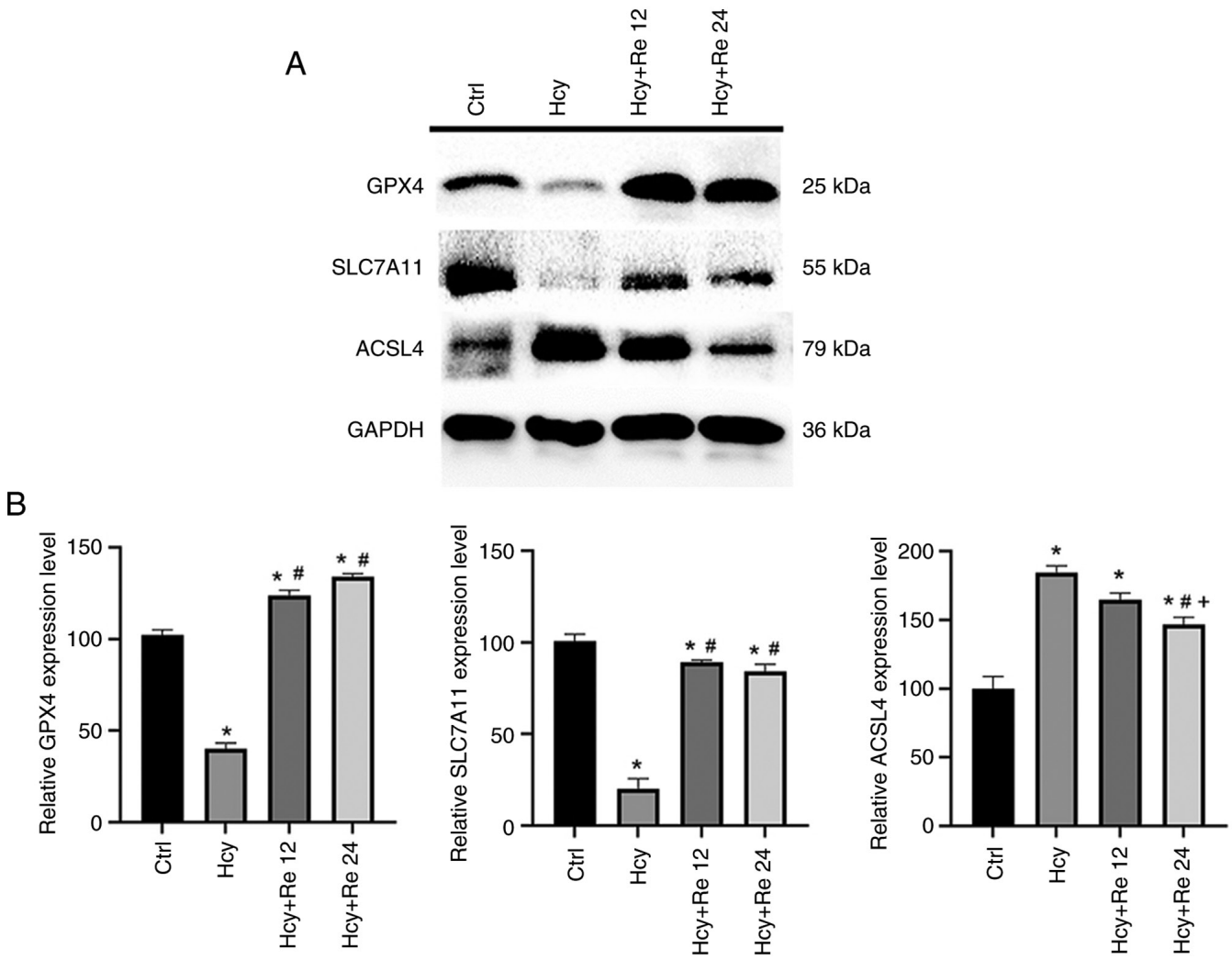

Figure 7. Effect of ginsenoside Re on the expression of proteins related to Hcy-induced ferroptosis in EA.hy926 cells. EA.hy926 cells were co-incubated with 2 mM Hcy, 2 mM Hcy + 12 μM ginsenoside Re or 2 mM Hcy + 24 μM ginsenoside Re for 24 h. (A) Representative bands and (B) analysis of protein levels of GPX4, SLC7A11 and ACSL4 determined by western blotting. The optical density of the proteins was calculated. Data are presented as the mean ± SD. *P<0.05 vs. Ctrl; $^{\#}$P<0.05 vs. Hcy; $^{+}$P<0.05 vs. Hcy + Re 12. GPX4, glutathione peroxidase 4; SLC7A11; solute carrier family 7 member 11; ACSL4, acyl-CoA synthetase long-chain family member 4; Hcy, homocysteine; Ctrl, control; Re, ginsenoside Re.

between ginsenoside Re and GPX4 at the MET-102 and LYS-99 residues is particularly notable, as this binding may stabilize GPX4, thereby enhancing its antioxidant capacity and reducing iron-dependent lipid peroxidation (49). Similarly, the binding of ginsenoside Re to ACSL4 at the residues ASP-66, ARG-60, GLY-523, GLN-524 and HIS-291 suggests that ginsenoside Re may interfere with ACSL4 function and inhibit its ferroptosis-promoting activity (50). Moreover, the interaction between ginsenoside Re and SLC7A11 at residues GLN-438, ASP-350 and ARG-440 may enhance the stability of SLC7A11, which is a key component of the system xc^- pathway and serves a central role in regulating ferroptosis (51). This hypothesis was verified by western blotting and cellular GSH assays. GPX4 and SLC7A11 expression levels and intracellular GSH levels were significantly decreased in the Hcy group. However, when compared with those in the Hcy group, GPX4 and SLC7A11 expression levels and intracellular GSH levels were significantly increased in the ginsenoside Re intervention groups. The present study suggested that Hcy impaired system xc-function and reduced GSH synthesis by decreasing SLC7A11 expression. By contrast, ginsenoside Re upregulated the expression of GPX4, increased the synthesis of GSH and reduced ferroptosis.

Ginsenoside Re has been shown to alleviate the inhibitory effect of miR-144-3p on SLC7A11 expression, resulting in the upregulation of SLC7A11. It was further confirmed that the solute carrier family 7 member 11 (SLC7A11) was the target gene of miR-144-3p by database analysis and western blotting (42). Specifically, miR-144-3p targets SLC7A11 mRNA, suppressing its translation and stability. Through modulation of miR-144-3p, ginsenoside Re indirectly enhances SLC7A11 expression, promoting cystine uptake and GSH synthesis (42). This cascade inhibits lipid peroxidation associated with ferroptosis. Elevated SLC7A11 levels increase GSH concentrations, which are key for the function of GPX4 as an antioxidant. Consequently, ginsenoside Re may indirectly augment GPX4 activity through SLC7A11-dependent mechanisms (42).

The pharmacokinetics and bioavailability of ginsenoside Re are the key limiting factors to its clinical application.

The oral bioavailability of ginsenoside Re is generally low, mainly due to its macromolecular structure and hydrophilic properties, which lead to intestinal malabsorption, rapid first-pass metabolism and enzyme-mediated degradation (52). A study showed that the use of ginsenoside Re complexes with polysaccharide protects ginsenoside Re from degradation through hydrogen bonding and regulates the expression of intestinal efflux proteins and tight junction proteins, thereby enhancing absorption and bioavailability (53). In animal experiments, ginsenoside Re has demonstrated rapid absorption and a relatively long elimination half-life. For example, after oral administration of red ginseng extract, ginsenoside Re has been detected as a 20(S)-protopanaxatriol saponin in mouse plasma. The high plasma protein binding and low hepatic distribution contribute to the prolonged plasma circulation time observed with highly glycosylated ginsenoside structures such as ginsenoside Re, which exhibits high plasma exposure; however, tetra- or tri-glycosylated saponins demonstrate greater accumulation susceptibility than ginsenoside Re, highlighting its metabolic uniqueness (54).

In conclusion, the present study indicated that ginsenoside Re may improve Hcy-induced ferroptosis in EA.hy926 cells by upregulating the expression of GPX4. Nevertheless, this established cell model may not fully replicate the dynamic functional adaptations characteristic of native endothelial cells within atherosclerotic microenvironments. Future *in vivo* studies are warranted to elucidate the therapeutic efficacy of ginsenoside Re in inhibiting endothelial ferroptosis.

Acknowledgements

Not applicable.

Funding

The present study was supported by the Clinical Research Fund project of Guangdong Medical Association (grant no. A202302018), the Medical Science and Technology Research Foundation of Guangdong Province (grant no. B2025385), the 'Hundred-Thousand-Million Project' for Science and Technology Support in 2025 (grant no. 250623211606897) and the Social Development Science and Technology Plan Project of Heyuan City (grant no. 250609171604668).

Availability of data and materials

The data generated in the present study may be requested from the corresponding author.

Authors' contributions

ShL, CZ, SY, SiL and SZ contributed to the conception and design of the present study. SL, CZ and SL wrote the manuscript and collected and analyzed the data. SL and SZ critically revised the final manuscript. KY and SY interpreted the data, and SL was responsible for capturing and organizing the images. SL, CZ, SY, KY, SZ and SL confirm the authenticity of all the raw data. All authors read and approved the final version of the manuscript.

Ethics approval and consent to participate

Not applicable.

Patient consent for publication

Not applicable.

Competing interests

The authors declare that they have no competing interests.

References

1. Duan H, Zhang Q, Liu J, Li R, Wang D, Peng W and Wu C: Suppression of apoptosis in vascular endothelial cell, the promising way for natural medicines to treat atherosclerosis. Pharmacol Res 168: 105599, 2021.
2. Qin X, Zhang J, Wang B, Xu G, Yang X, Zou Z and Yu C: Ferritinophagy is involved in the zinc oxide nanoparticles-induced ferroptosis of vascular endothelial cells. Autophagy 17: 4266-4285, 2021.
3. Yang Z, Shi J, Chen L, Fu C, Shi D and Qu H: Role of pyroptosis and ferroptosis in the progression of atherosclerotic plaques. Front Cell Dev Biol 10: 811196, 2022.
4. Carlson BA, Tobe R, Yefremova E, Tsuji PA, Hoffmann VJ, Schweizer U, Gladyshev VN, Hatfield DL and Conrad M: Glutathione peroxidase 4 and vitamin E cooperatively prevent hepatocellular degeneration. Redox Biol 9: 22-31, 2016.
5. Imai H and Nakagawa Y: Biological significance of phospholipid hydroperoxide glutathione peroxidase (PHGPx, GPx4) in mammalian cells. Free Radic Biol Med 34: 145-169, 2003.
6. Tang D, Chen X, Kang R and Kroemer G: Ferroptosis: Molecular mechanisms and health implications. Cell Res 31: 107-125, 2021.
7. Illés E, Patra SG, Marks V, Mizrahi A and Meyerstein D: The Fe(II)(citrate) Fenton reaction under physiological conditions. J Inorg Biochem 206: 111018, 2020.
8. Kist M and Vucic D: Cell death pathways: Intricate connections and disease implications. EMBO J 40: e106700, 2021.
9. Kagan VE, Mao G, Qu F, Angeli JP, Doll S, Croix CS, Dar HH, Liu B, Tyurin VA, Ritov VB, *et al*: Oxidized arachidonic and adrenic PEs navigate cells to ferroptosis. Nat Chem Biol 13: 81-90, 2017.
10. Dixon SJ, Lemberg KM, Lamprecht MR, Skouta R, Zaitsev EM, Gleason CE, Patel DN, Bauer AJ, Cantley AM, Yang WS, *et al*: Ferroptosis: An iron-dependent form of nonapoptotic cell death. Cell 149: 1060-1072, 2012.
11. Bai T, Li M, Liu Y, Qiao Z and Wang Z: Inhibition of ferroptosis alleviates atherosclerosis through attenuating lipid peroxidation and endothelial dysfunction in mouse aortic endothelial cell. Free Radic Biol Med 160: 92-102, 2020.
12. Huang D, Zheng S, Liu Z, Zhu K, Zhi H and Ma G: Machine learning revealed ferroptosis features and a novel ferroptosis-based classification for diagnosis in acute myocardial infarction. Front Genet 13: 813438, 2022.
13. Tang LJ, Zhou YJ, Xiong XM, Li NS, Zhang JJ, Luo XJ and Peng J: Ubiquitin-specific protease 7 promotes ferroptosis via activation of the p53/TfR1 pathway in the rat hearts after ischemia/reperfusion. Free Radic Biol Med 162: 339-352, 2021.
14. Guo Y, Zhang W, Zhou X, Zhao S, Wang J, Guo Y, Liao Y, Lu H, Liu J, Cai Y, *et al*: Roles of ferroptosis in cardiovascular diseases. Front Cardiovasc Med 9: 911564, 2022.
15. Chen X, Xu S, Zhao C and Liu B: Role of TLR4/NADPH oxidase 4 pathway in promoting cell death through autophagy and ferroptosis during heart failure. Biochem Biophys Res Commun 516: 37-43, 2019.
16. Stockwell BR, Friedmann Angeli JP, Bayir H, Bush AI, Conrad M, Dixon SJ, Fulda S, Gascón S, Hatzios SK, Kagan VE, *et al*: Ferroptosis: A regulated cell death nexus linking metabolism, redox biology, and disease. Cell 171: 273-285, 2017.
17. Forcina GC and Dixon SJ: GPX4 at the crossroads of lipid homeostasis and ferroptosis. Proteomics 19: e1800311, 2019.
18. Shimada K, Skouta R, Kaplan A, Yang WS, Hayano M, Dixon SJ, Brown LM, Valenzuela CA, Wolpaw AJ and Stockwell BR: Global survey of cell death mechanisms reveals metabolic regulation of ferroptosis. Nat Chem Biol 12: 497-503, 2016.

19. Dixon SJ, Patel DN, Welsch M, Skouta R, Lee ED, Hayano M, Thomas AG, Gleason CE, Tatonetti NP, Slusher BS and Stockwell BR: Pharmacological inhibition of cystine-glutamate exchange induces endoplasmic reticulum stress and ferroptosis. Elife 3: e02523, 2014.
20. Kim J, Kim H, Roh H and Kwon Y: Causes of hyperhomocysteinemia and its pathological significance. Arch Pharm Res 41: 372-383, 2018.
21. Qin X, Xu M, Zhang Y, Li J, Xu X, Wang X, Xu X and Huo Y: Effect of folic acid supplementation on the progression of carotid intima-media thickness: A meta-analysis of randomized controlled trials. Atherosclerosis 222: 307-313, 2012.
22. Esse R, Barroso M, Tavares de Almeida I and Castro R: The contribution of homocysteine metabolism disruption to endothelial dysfunction: State-of-the-art. Int J Mol Sci 20: 867, 2019.
23. Zhang X, Huang Z, Xie Z, Chen Y, Zheng Z, Wei X, Huang B, Shan Z, Liu J, Fan S, *et al*: Homocysteine induces oxidative stress and ferroptosis of nucleus pulposus via enhancing methylation of GPX4. Free Radic Biol Med 160: 552-565, 2020.
24. Mancuso C and Santangelo R: Panax ginseng and Panax quinquefolius: From pharmacology to toxicology. Food Chem Toxicol 107: 362-372, 2017.
25. Quan HY, Yuan HD, Jung MS, Ko SK, Park YG and Chung SH: Ginsenoside Re lowers blood glucose and lipid levels via activation of AMP-activated protein kinase in HepG2 cells and high-fat diet fed mice. Int J Mol Med 29: 73-80, 2012.
26. Kim JM, Park CH, Park SK, Seung TW, Kang JY, Ha JS, Lee DS, Lee U, Kim DO and Heo HJ: Ginsenoside Re ameliorates brain insulin resistance and cognitive dysfunction in high fat diet-induced C57BL/6 mice. J Agric Food Chem 65: 2719-2729, 2017.
27. Wang H, Lv J, Jiang N, Huang H, Wang Q and Liu X: Ginsenoside Re protects against chronic restraint stress-induced cognitive deficits through regulation of NLRP3 and Nrf2 pathways in mice. Phytother Res 35: 2523-2535, 2021.
28. Su F, Xue Y, Wang Y, Zhang L, Chen W and Hu S: Protective effect of ginsenosides Rg1 and Re on lipopolysaccharide-induced sepsis by competitive binding to Toll-like receptor 4. Antimicrob Agents Chemother 59: 5654-5663, 2015.
29. Wang QW, Yu XF, Xu HL, Zhao XZ and Sui DY: Ginsenoside Re improves isoproterenol-induced myocardial fibrosis and heart failure in rats. Evid Based Complement Alternat Med 2019: 3714508, 2019.
30. Yao H, Li J, Song Y, Zhao H, Wei Z, Li X, Jin Y, Yang B and Jiang J: Synthesis of ginsenoside Re-based carbon dots applied for bioimaging and effective inhibition of cancer cells. Int J Nanomedicine 13: 6249-6264, 2018.
31. Lee GH, Lee WJ, Hur J, Kim E, Lee HG and Seo HG: Ginsenoside Re mitigates 6-hydroxydopamine-induced oxidative stress through upregulation of GPX4. Molecules 25: 188, 2020.
32. Shi J, Chen D, Wang Z, Li S and Zhang S: Homocysteine induces ferroptosis in endothelial cells through the systemXc$^-$/GPX4 signaling pathway. BMC Cardiovasc Disord 23: 316, 2023.
33. Yang R, Gao W, Wang Z, Jian H, Peng L, Yu X, Xue P, Peng W, Li K and Zeng P: Polyphyllin I induced ferroptosis to suppress the progression of hepatocellular carcinoma through activation of the mitochondrial dysfunction via Nrf2/HO-1/GPX4 axis. Phytomedicine 122: 155135, 2024.
34. Wu B, Lan X, Chen X, Wu Q, Yang Y and Wang Y: Researching the molecular mechanisms of Taohong Siwu Decoction in the treatment of varicocele-associated male infertility using network pharmacology and molecular docking: A review. Medicine (Baltimore) 102: e34476, 2023.
35. Gimbrone MA Jr and García-Cardeña G: Endothelial cell dysfunction and the pathobiology of atherosclerosis. Circ Res 118: 620-636, 2016.
36. Botts SR, Fish JE and Howe KL: Dysfunctional vascular endothelium as a driver of atherosclerosis: Emerging insights into pathogenesis and treatment. Front Pharmacol 12: 787541, 2021.
37. Mou Y, Wang J, Wu J, He D, Zhang C, Duan C and Li B: Ferroptosis, a new form of cell death: Opportunities and challenges in cancer. J Hematol Oncol 12: 34, 2019.
38. Ouyang S, You J, Zhi C, Li P, Lin X, Tan X, Ma W, Li L and Xie W: Ferroptosis: The potential value target in atherosclerosis. Cell Death Dis 12: 782, 2021.
39. Azad MAK, Huang P, Liu G, Ren W, Teklebrh T, Yan W, Zhou X and Yin Y: Hyperhomocysteinemia and cardiovascular disease in animal model. Amino Acids 50: 3-9, 2018.
40. Shi Q, Liu R and Chen L: Ferroptosis inhibitor ferrostatin-1 alleviates homocysteine-induced ovarian granulosa cell injury by regulating TET activity and DNA methylation. Mol Med Rep 25: 130, 2022.
41. Wang Y, Kuang X, Yin Y, Han N, Chang L, Wang H, Hou Y, Li H, Li Z, Liu Y, *et al*: Tongxinluo prevents chronic obstructive pulmonary disease complicated with atherosclerosis by inhibiting ferroptosis and protecting against pulmonary microvascular barrier dysfunction. Biomed Pharmacother 145: 112367, 2022.
42. Ye J, Lyu TJ, Li LY, Liu Y, Zhang H, Wang X, Xi X, Liu ZJ and Gao JQ: Ginsenoside Re attenuates myocardial ischemia/reperfusion induced ferroptosis via miR-144-3p/SLC7A11. Phytomedicine 113: 154681, 2023.
43. Yang WS, Kim KJ, Gaschler MM, Patel M, Shchepinov MS and Stockwell BR: Peroxidation of polyunsaturated fatty acids by lipoxygenases drives ferroptosis. Proc Natl Acad Sci USA 113: E4966-E4975, 2016.
44. Chen Y, Deng Y, Chen L, Huang Z, Yan Y and Huang Z: miR-16-5p regulates ferroptosis by targeting SLC7A11 in adriamycin-induced ferroptosis in cardiomyocytes. J Inflamm Res 16: 1077-1089, 2023.
45. Xu S, Wu B, Zhong B, Lin L, Ding Y, Jin X, Huang Z, Lin M, Wu H and Xu D: Naringenin alleviates myocardial ischemia/reperfusion injury by regulating the nuclear factor-erythroid factor 2-related factor 2 (Nrf2)/System xc-/glutathione peroxidase 4 (GPX4) axis to inhibit ferroptosis. Bioengineered 12: 10924-10934, 2021.
46. Zhang L, Liu W, Liu F, Wang Q, Song M, Yu Q, Tang K, Teng T, Wu D, Wang X, *et al*: IMCA induces ferroptosis mediated by SLC7A11 through the AMPK/mTOR pathway in colorectal cancer. Oxid Med Cell Longev 2020: 1675613, 2020.
47. Wang L, Liu Y, Du T, Yang H, Lei L, Guo M, Ding HF, Zhang J, Wang H, Chen X and Yan C: ATF3 promotes erastin-induced ferroptosis by suppressing system Xc. Cell Death Differ 27: 662-675, 2020.
48. Parker JL, Deme JC, Kolokouris D, Kuteyi G, Biggin PC, Lea SM and Newstead S: Molecular basis for redox control by the human cystine/glutamate antiporter system xc. Nat Commun 12: 7147, 2021.
49. Qiao O, Zhang L, Han L, Wang X, Li Z, Bao F, Hao H, Hou Y, Duan X, Li N and Gong Y: Rosmarinic acid plus deferasirox inhibits ferroptosis to alleviate crush syndrome-related AKI via Nrf2/Keap1 pathway. Phytomedicine 129: 155700, 2024.
50. Ren S, Wang J, Dong Z, Li J, Ma Y, Yang Y, Zhou T, Qiu T, Jiang L, Li Q, *et al*: Perfluorooctane sulfonate induces ferroptosis-dependent non-alcoholic steatohepatitis via autophagy-MCU-caused mitochondrial calcium overload and MCU-ACSL4 interaction. Ecotoxicol Environ Saf 280: 116553, 2024.
51. Wei XL, Yu AG, Zhang X, Pantopoulos K, Liu ZB, Xu PC, Zheng H and Luo Z: Fe_2O_3 nanoparticles induce ferroptosis by binding to the N-terminus of ACSL4 and suppressing its ubiquitin-mediated degradation. Free Radic Biol Med 238: 123-136, 2025.
52. Cai J, Huang K, Han S, Chen R, Li Z, Chen Y, Chen B, Li S, Xinhua L and Yao H: A comprehensive system review of pharmacological effects and relative mechanisms of Ginsenoside Re: Recent advances and future perspectives. Phytomedicine 102: 154119, 2022.
53. Zhu Y, Yue J, Yan R, Xia W, Li T and Fu X: Enhancement in the intestinal absorption of ginsenoside Re by ginseng polysaccharides and its mechanisms. Food Chem 488: 144914, 2025.
54. Jeon JH, Lee J, Choi MK and Song IS: Pharmacokinetics of ginsenosides following repeated oral administration of red ginseng extract significantly differ between species of experimental animals. Arch Pharm Res 43: 1335-1346, 2020.